SOCIAL NEUROSCIENCE, 2015
http://dx.doi.org/10.1080/17470919.2015.1056883

Modeling the neurodynamic organizations and interactions of teams

Ronald H. Stevens[1,2] and Trysha L. Galloway[2]

[1]UCLA School of Medicine, Los Angeles, CA, USA
[2]The Learning Chameleon, Inc., Los Angeles, CA, USA

Across-brain neurodynamic organizations arise when teams perform coordinated tasks. We describe a symbolic electroencephalographic (EEG) approach that identifies when team neurodynamic organizations occur and demonstrate its utility with scientific problem solving and submarine navigation tasks. Each second, neurodynamic symbols (NS) were created showing the 1–40 Hz EEG power spectral densities for each team member. These data streams contained a performance history of the team's across-brain neurodynamic organizations. The degree of neurodynamic organization was calculated each second from a moving window average of the Shannon entropy over the task. Decreased NS entropy (i.e., greater neurodynamic organization) was prominent in the ~16 Hz EEG bins during problem solving, while during submarine navigation, the maximum NS entropy decreases were ~10 Hz and were associated with establishing the ship's location. Decreased NS entropy also occurred in the 20–40 Hz bins of both teams and was associated with uncertainty or stress. The highest mutual information levels, calculated from the EEG values of team dyads, were associated with decreased NS entropy, suggesting a link between these two measures. These studies show entropy and mutual information mapping of symbolic EEG data streams from teams can be useful for identifying organized across-brain team activation patterns.

Keywords: Team neurodynamics; Synchrony; EEG; Entropy; Mutual information teamwork.

Most organizations could benefit from a deeper understanding of the fluctuating dynamics of their teams. Teams and teamwork are seldom static entities as teams need to adapt to the continually changing environmental constraints. With high-performing teams in rapidly evolving environments, the changing dynamics can outpace conventional approaches for understanding them (Wildman, Salas, & Scott, 2014), and it is not always clear how to modify teams or training in response. The challenges facing organizations are compounded by the need for training solutions that are cost-effective, highly automated, adaptable, and capable of producing quantifiable behavioral changes in teams that are indicative of deep learning.

Teamwork research has historically focused on macro-level concepts like team effectiveness (Salas, Stagl, & Burke, 2004) or resilience (Hollnagel, 2009). In recent years, the interest has shifted toward the dynamics within the neurodynamic, cognitive and behavioral data streams that are being collected in natural settings (Gorman, Amazeen, & Cooke, 2010;

Correspondence should be addressed to: Ronald H. Stevens, 5601 W. Slauson Ave, #184, Culver City, CA 90230, USA.
E-mail: ron@teamneurodynamics.com

The authors thank Marcia Sprang, Ph.D., and the students at Esperanza High School for their assistance with the Map Task studies. The authors also thank Veasna Tan and Bradly Stone from Advanced Brain Monitoring, Inc. for their assistance with EEG data collection and processing. Special thanks to Thomas Wohlgemuth and Lt. Robert Buckles at the Submarine Learning Center in Groton, CT, for their help with the on-site logistics for the SPAN studies.

No potential conflict of interest was reported by the authors.

This work is supported in part by the Defense Advanced Projects Agency [contract number W31P4Q-12-C-0166] and National Science Foundation SBIR [grant numbers IIP-1215, IIP-121527, IIP 0822020, and IIP 1215327].

Onken, Chamanthi, Karunasekara, Kayser, & Panzeri, 2014; Stevens, Galloway, Wang, & Berka, 2012).

One approach for understanding the meso- and micro-scale temporal dynamics of teams emerges from the neurodynamically linked concepts of brain wave synchronization (Will & Berg, 2007) and across-brain social couplings (Hasson, Ghazanfar, Glantucci, Garrod, & Keysers, 2011). It is well established that some electrical rhythms of the brain synchronize to external repetitive sounds/images (Adrian & Matthews, 1934; Galambos, Makeig, & Talmachoff, 1981). These synchronizations can be simple reflections of the periodicity of the stimulus sequence or may include rhythms corresponding to the preferred rates of perceptomotor behaviors like the production of, or listening to music, finger tapping, or sentence comprehension (Moreno, De Vega, & León, 2013; Van Noorden & Moelants, 1999). These findings were extended by Hasson, Nir, Levy, Fuhrmann, and Malach (2004) to a more complex situation by having individuals view scenes from a movie. As the video unfolded, the embedded visual and auditory elements entrained the subjects' cognition with inter-subject synchronizations occurring in the visual, auditory, and cortical brain regions. The complex nature of the stimuli in these studies suggested that teams performing complex tasks might exhibit neurodynamic entrainments similar to those of individuals watching a movie.

Teams differ from individuals viewing a movie in that they help shape the storyline by participating as part of a complex adaptive system that influences, and is influenced by, other complex adaptive systems like their teammates, the environment, and other complex systems with their own sets of teams. Nevertheless, based on prior brain wave studies, individuals in teams might be expected to respond similarly to important events unfolding during the task. If so, systems could be developed that would identify when neurodynamic relationships between team members entered a coupled state as a result of the unfolding situation and their teammates' actions. This state may then persist until a sufficient change in team/task status leads the team out of this organized state into a new one. The information contained in these neurodynamic organizations may then be extracted to support the creation of new measurement systems for understanding team formation, training, and performance.

Neurophysiological measures of social coordination like those described by Tognoli and Kelso (2013) are obvious choices for developing such models. Using high-spectral electroencephalography (EEG) over short time scales (e.g., 1–5 s), these investigators have described multiple neuromarkers of social coordination in the 9–12 Hz frequency range. These markers include the 10.9 Hz phi complex, which is modulated by intentional coordination (Tognoli, Lagarde, De Guzman, & Kelso, 2007), and the medial left and right mu EEG components in the alpha (9–11 Hz) and beta (~15–20 Hz) frequencies, which may represent activities associated with the human mirror neuron system (Oberman, Pineda, & Ramachandran, 2008; Pineda, 2008).

The phenomena of cross-frequency phase synchrony, (Palva & Palva, 2007) and nested oscillations (Canolty et al., 2006) are also potential contributors to team neurodynamic organizations as they are strong contributors to communication, coordination, and working memory in individuals (Fries, 2005).

The goal of this study was to determine the types of inferences that can be made about team–task interactions from their changing neurodynamic organizations. We begin by presenting a symbolic entropy modeling approach, based on EEG power spectral densities, for identifying periods of increased team neurodynamic organization within the 1–40 Hz EEG frequency spectrum and across the scalp. Next, we explored the across-task generality of symbolic modeling by contrasting the dynamics on two types of single-trial natural tasks using quantitative information-based measures. These tasks included a map navigation task (MT) where dyads of high school students communicated by speech to co-navigate through a series of map landmarks. The second task was a required high-fidelity navigation simulation for five-person US Navy submarine navigation teams.

METHODS

Tasks

Map task

When performing the Human Communication Research Center's MT, team members faced each other while viewing a computer displaying a map with multiple landmarks (Doherty-Sneddon et al., 1997). The two maps were similar but not identical and students could not see each other's map. The instruction giver (Giver, abbreviated G), had a printed path through the landmarks and verbally guided the follower (Follower, abbreviated F) in duplicating that path on his/her computer by drawing the line with a mouse (Figure 1). Occasionally, the mouse drawing

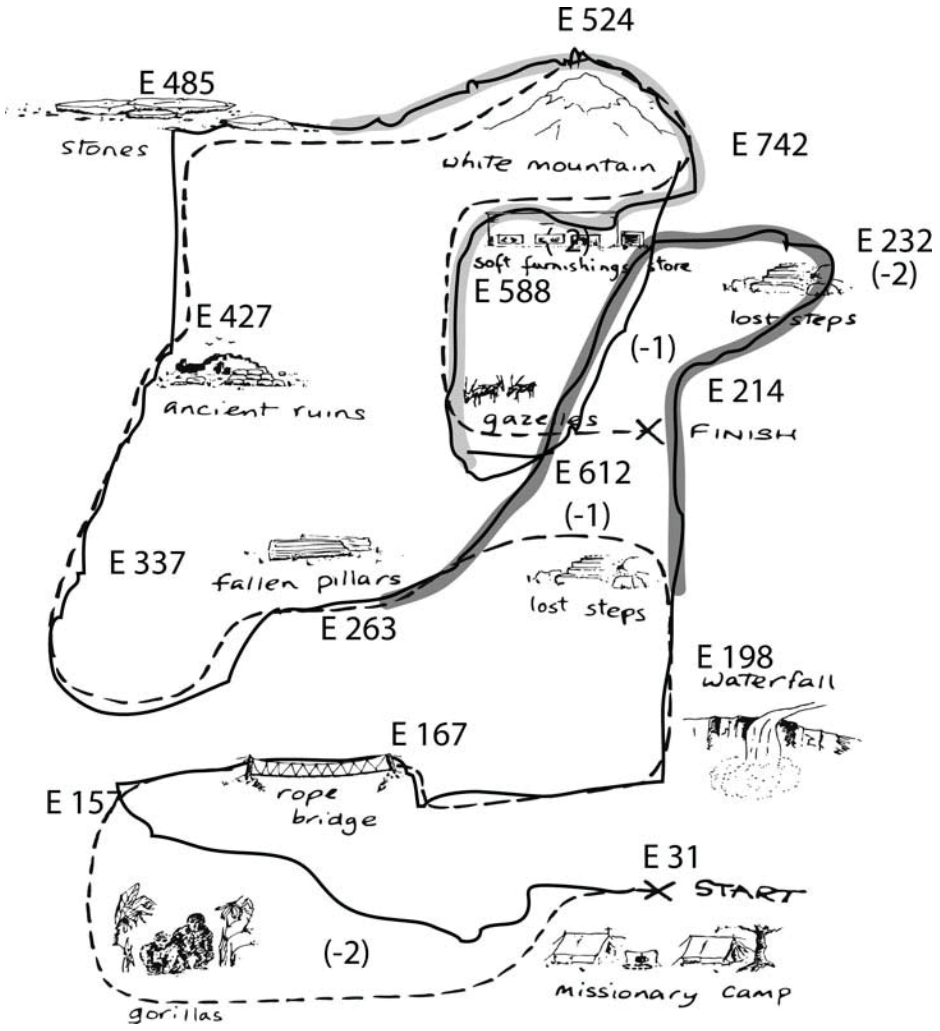

Figure 1. Sample MT performance (#G3S1). The dotted line indicates the target path on the G's map; the solid line shows the F's trace. The performance times (seconds) are marked at different locations, i.e., E 167. There are two segments of the traced path highlighted in dark gray (~210–250 s) and light gray (~500–600 s) that represent periods of increased MI as described in the text. These periods are also highlighted in the drawing transactions in Figure 6c.

was delayed due to the microprocessor overload caused by both the EEG acquisitions and the video recording, and during these delays, the users often repeatedly clicked the mouse. Segments with large numbers of mouse clicks are easily visualized and served as markers for this unintended task perturbation.

Students completed the MT using dialog that was unscripted, fluent, and contained easily identified goals. Multiple G-F speech exchanges were needed to draw the path between any two landmarks; in the figures, these series of speech exchanges are aggregated into what are termed transactions. Each transaction had little dependency on prior transactions, accomplishments, or decisions.

Seven dyads of eleventh and twelfth grade students enrolled in advanced placement chemistry courses were the experimental subjects for the MT; they received no specific training prior to beginning the task and no performance feedback was provided to the teams either during or after the task. Informed consent was obtained from the parents allowing the students to participate in the study and to have their images and speech made available for additional research analysis.

Submarine piloting and navigation

Submarine piloting and navigation (SPAN) simulations were required exercises for Junior Officers in the

Submarine Officer Advanced Candidacy course at the US Navy Submarine School. SPAN sessions contained three training segments: briefing, scenario, and debriefing. Briefing was where the team reviewed the environmental conditions and other ships in the area, and statically established the submarine's position. The scenario was the training part of the navigation simulation where events included encounters with approaching ships, the need to avoid shoals, changing weather conditions, and instrument failure. One team process in the scenario required updating the ship's position every three minutes. In this process, called "rounds," three navigation landmarks were chosen and their visual or electronic bearings from the boat were measured and plotted on a chart. The regular "rounds" sequence usually began with a "1 min to next round" announcement, followed by a "mark the round" call 60 s later. The observations were made, verified with the estimated position and depth of the water, and then the call to "end round" was made. The debriefing was an after-action review where all team members participated in critical performance discussions.

The experimental SPAN teams included five crew members: the navigator (NV); the officer on deck (OD); the contact manager (CM), who kept track of other ship traffic; the quartermaster (QM), who maintained the ship's position; and the radar operator (RD) (other people were "satellite" team members but were not directly involved in the team processes analyzed here).

Electroencephalography

The X-10 wireless headsets from Advanced Brain Monitoring, Inc. (Carlsbad, CA, USA) were used for data collection. This wireless EEG headset system included sensor site locations: F3, F4, C3, C4, P3, P4, Fz, Cz, POz in a monopolar configuration referenced to linked mastoids; bipolar derivations were included that have been reported to reflect sensorimotor activity (FzC3) (Wang, Hong, Gao, & Gao, 2007), workload (F3Cz, C3C4) (Roux & Uhlhaas, 2014) and alpha wave components of the human mirror neuron system (Oberman et al., 2008). Embedded within the EEG data stream from each team member were eye blinks that were automatically detected and decontaminated using interpolation algorithms contained in the EEG acquisition software (Berka et al., 2004). These interpolations represented ~5% of the simulation time and in previous studies have not significantly influenced the detection of team neurophysiological activities that occurred throughout the performances (Stevens & Galloway, 2014; Stevens et al., 2012). The EEG power spectral density (PSD) values were computed each second at each sensor for the 1–40 Hz frequency bins by the B-Alert Lab PSD Analysis software (Carlsbad, CA, USA).

Symbolic neurodynamic data modeling

The goal was to develop neurodynamic data streams that had internal structure(s) with temporal information about the organization, function, and performance of teams. A symbolic approach was used to develop these data streams where the raw EEG data streams of team members were combined into one composite complex-valued measure of team organization around a neurophysiological measure. While illustrated for MT dyads, the process was similar for teams of 3–6 persons, including SPAN teams (Stevens, Gorman, Amazeen, Likens, & Galloway, 2013).

The simple averaging of an EEG marker (i.e., power levels at a frequency) across members of a team could be one starting point for modeling team neurodynamics, and may be particularly useful when searching for when all team members had elevated or depressed levels of the marker. The limitation of this approach is that the relationships between team members, their individual roles, and the immediate perceptual context do not factor into the aggregate. Also, periods where all team members had high or low marker levels are infrequent (Kolm, Stevens, & Galloway, 2013) and focusing on them would ignore the other synergistic links between team members expected at the neurodynamic level. Treating data from multiple time series as symbols is another approach that has been used for discovering interesting data patterns in temporal data streams (Daw, Finney, & Tracy, 2003; Lin, Keogh, Lonardi, & Chiu, 2003). Below we describe the process of symbol generation for dyads performing MT simulations; the procedure for SPAN crews is similar, but the number of symbols was expanded to 25 to accommodate the EEG PSD values across the different team members (Stevens et al., 2013).

To generate neurodynamic symbols (NS), each second we equated the absolute levels of one EEG PSD frequency bin (i.e., 40 Hz) of a team member with his/her own average levels over the period of the particular task. This identified whether an individual team member was experiencing above- or below-average levels of an EEG marker and whether the team as a whole was experiencing above or below levels. Classifying the set of symbols over entire MT or SPAN performances (i.e., including briefing and debriefing segments) provided neurodynamic models

encompassing a comprehensive set of task situations/loads (Fishel, Muth, & Hoover, 2007).

As previously described (Stevens et al., 2013), in this process the EEG PSD levels were partitioned into the upper 33%, the lower 33%, and the middle 33%, which were assigned values of 3, −1, and 1, respectively. The next step combined these values at each second for each team member into a vector, which was classified by a pretrained artificial neural network and assigned a symbol number. We used an unsupervised ANN architecture with 9–100 output nodes depending on the task and the team. In previous studies, we have compared the sensitivity of single-trial ANN versus heterologous networks by wavelet analysis; use of the heterologous networks decreased the temporal resolution to task events by 5–10 s (Stevens, Galloway, Wang, Berka, & Behneman, 2011). The symbols created showed the EEG PSD levels for each person in the team and situated them in the context of the levels of the other team member(s) as well as within the immediate context of the task. These symbol combinations also represent the probability distribution of the team's response to the ongoing task stimuli.

The symbol from one MT dyad shown in Figure 2a represented a state where the 40 Hz EEG PSD spectral band power of G was high and that of F was low. The nine-symbol state space of the possible dyad combinations is shown in Figure 2b. The resulting performance data was a linear sequence of symbols, one for each second of the task. Quantitative estimates of symbol distribution along the data stream were made by calculating the Shannon entropy (Shannon & Weaver, 1949). This procedure was then repeated for each of the 39 remaining EEG PSD bins, and across the EEG monopole and bipolar electrodes to create three-dimensional neurodynamic entropy maps plotting entropy versus simulation time and EEG PSD frequency.

The temporal expression of these symbols during an MT performance is shown in Figure 2c. The rows show when each of the nine NS symbols in Figure 2b were expressed. During the first 100 s, NS #2 and 3 appeared more often than NS #7–9. By referencing Figure 2b, this indicated that G was expressing high 40 Hz EEG power levels while F was expressing average to low levels. Around 200 s, the NS distribution changed with NS #1–5 no longer being expressed and being sequentially replaced by NS #6, with both members having low power levels, and then NS #8, a state where G expressed low power levels while F expressed high levels. This coincided with F having difficulty drawing the map on the computer with the mouse as shown by the increased density of the mouse clicks (Figure 2d).

The line in Figure 2c shows quantitative estimates of these changing symbol dynamics. These estimates were calculated and quantitated by measuring the Shannon entropy,

$$\text{NS entropy} = -\sum_{i=1}^{\#\text{NS States}} p_i \cdot \log p_i, \qquad (1)$$

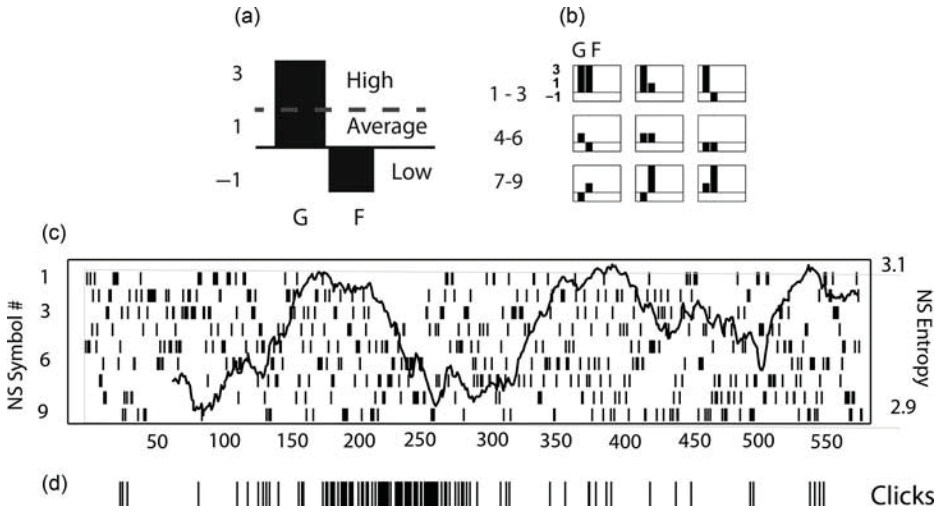

Figure 2. Neurodynamic symbol generation and expression. (a) This symbol represented times when G had above-average levels of 40 Hz EEG spectral power and F had below-average levels. (b) The nine-symbol state space for the MT experiments. (c) Second-by-second expression of the nine neurodynamic symbols in the 40 Hz PSD bin; the trace indicates the NS entropy levels over a 60 s moving window. (d) Mouse clicks of the F; the increased density from 150 to 300 s indicated a period of drawing difficulties.

where p_i is the relative frequency of NS state i over a sliding 60 s window; the entropy was first measured over the initial 60 s. Then at subsequent seconds the window was shifted, removing the first symbol and appending a new one at the end; the entropy was then recalculated. Performance segments with restricted symbol expression had lower entropy levels, while segments with greater symbol diversity had higher entropy. As reference points, the Shannon entropy value for nine symbols is 3.17, while if only six symbols were expressed, the entropy value would drop to 2.58.

Surrogate data testing was used in all experiments where the NS data streams were randomized before the Shannon entropy was calculated; this significantly increased the NS entropy (3.05 ± .02 vs. 3.12 ± .003, $df = 15$, $T = -8.6$, $p < .001$).

NS entropy is therefore the measure of a neurophysiological organizational process that results in a prolonged and restricted relationship(s) between EEG PSD levels of team members. In this context, periods of decreased entropy reflected increased neurodynamic organization. This relationship may exist for only a single EEG PSD frequency bin or more globally across multiple PSD frequency bins.

It is important to reiterate that team NS entropy levels do not necessarily reflect the mean EEG PSD levels of the teammates. Instead, the symbolic modeling emphasizes times when the EEG PSD levels of G and F had a restricted relationship over a prolonged time period. These may be times when low NS entropy at a particular frequency resulted from either high or low EEG PSD levels for both team members, but they could also result from other combinatorial possibilities. It is also important to reiterate that the neurodynamic fluctuations may vary greatly from one PSD frequency bin to the next.

These ideas are illustrated in Figure 3 where the entropy fluctuations of the NS symbols at 16 Hz (Figure 3a) and 20 Hz (Figure 3b) PSD frequency bins were compared. From the performance start until ~200 s, the team alternated between G having high and F low (NS #3), and the F having high and G having low 16 Hz levels (NS #8 and 9). Then from ~500 s to the task end, the major NS expressions were #5 and 6, i.e., both team members with below-average 16 Hz power. Between these times, there was more heterogeneous symbol expression. Similar organizations were not seen in the 20 Hz band (Figure 3b) showing the EEG frequency specificity.

The same procedure was used for constructing the five-person SPAN team vectors and symbols, the exception being the use of 25 rather than 9 neural network output symbols. This increase in the symbol state space from 9 to 25 raised the maximum possible NS entropy level to 4.64 (i.e., $\log_2$ (25)).

Mutual information of team dyads

The fluctuations in the NS entropy identify periods of changing team neurodynamic organization but they provide little information about the possible roles that synergistic interactions among the team members play in these organizations; mutual information (MI) descriptions help supply this data. MI is a quantity that measures the mutual dependence of two variables. MI has been widely used for evaluating information representations, transmissions, and content in single

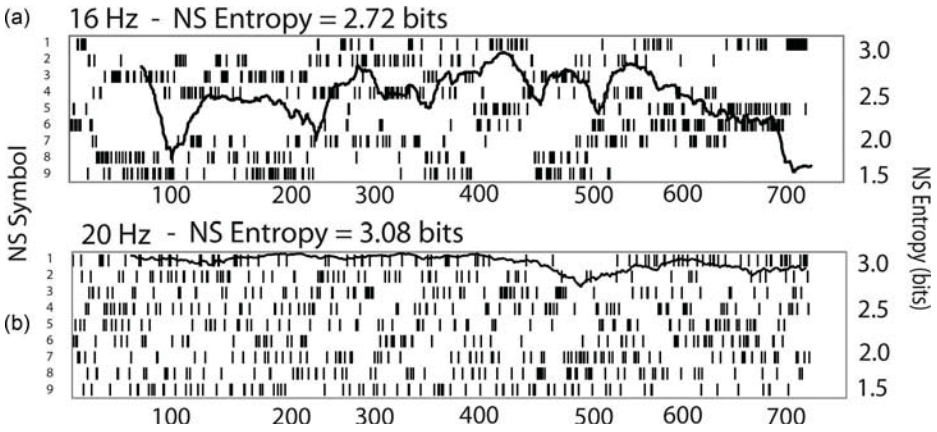

Figure 3. (a) The NS in the 16 Hz and (b) the 20 Hz PSD frequency bins were plotted each second (left scale); the tracings indicate the NS entropy levels (right scale).

neuron or populations of neurons stimulus- responses paradigms (Onken et al., 2014; Schneidman, Bialek, & Berry, 2003), as well as for reverse engineering gene regulatory and other complex networks (Villaverde, Ross, Moran, & Banga, 2014). We wished to determine whether MI could complement NS entropy measures for understanding the structure of interactions between team members from the neurodynamic data. Two different sources of symbols were used for calculating MI in our studies. For the MT dyads, or for dyads constructed from the five crew members in SPAN, the EEG PSD state representations (i.e., −1, 1, and 3) described in Figure 2 were used symbolically. In SPAN studies where the MI was calculated between two pairs of crew members, we used the 25 NS state space symbols. In all studies, a moving-average window approach for MI data reporting was used as described above for NS entropy to directly compare the temporal changes and to relate the two measures to task events.

RESULTS

EEG frequency and NS entropy profiles

The variability of team NS entropy across the EEG PSD spectrum was determined for MT (Figure 4a) and SPAN team performances (Figure 4b). The major organizational locus for MT teams was in the 15–17 Hz PSD bins, while for SPAN teams it was in the 9–11 Hz bins. For both tasks, there was a downward trend in NS entropy with increasing frequency indicating additional organizations in the high beta/low gamma regions.

For the MT performances, the lowest total NS entropy and the 16 Hz EEG NS entropy levels occurred when measured at the FzC3 and C3C4 sensor channels. For SPAN team performances, the lowest total NS entropy levels were again seen at the FzC3 and C3C4 sensor channels, but at the 10 Hz EEG band, the largest NS entropy decreases occurred when measured at the FzP0 and CzP0 sensor channels; the difference was significant when compared with the FzC3 and C3C4 sensor channels (4.32 ± .016 vs. 4.29 ± .017, $df = 12$, $T = -2.4$, $p < .04$). The results also suggest the differential involvement of brain regions and EEG frequencies in team neurodynamic organizations.

The team-averaged raw EEG power spectra for the MT (Figure 4e) and SPAN teams (Figure 4f) were calculated by averaging the PSD from each of the team members at each EEG frequency bin; the spectra profiles were similar for both sets of teams.

Neurodynamic entropy maps: MT

To easily visualize the temporal and frequency relationships of neurodynamic entropy expression, models were developed for individual team performances where the NS entropy was plotted each second versus the forty 1 Hz PSD frequency bins (Figure 5). When viewed as a contour map from above, the periods of decreased NS entropy (i.e., increased team neurodynamic organization) appeared as darkened contours. These periods could then be related to team activities

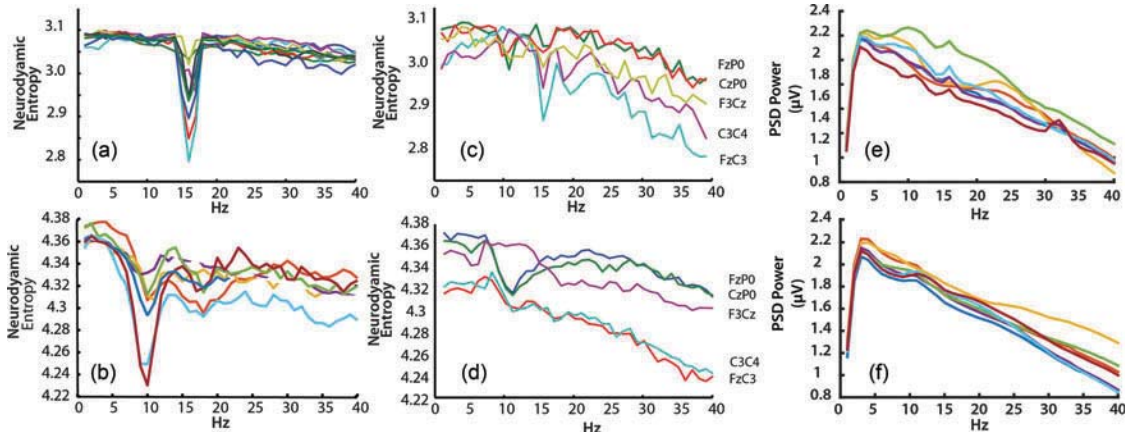

Figure 4. Plot of NS entropy versus EEG PSD bins for (a) MT ($n = 7$) and (b) SPAN ($n = 7$) teams. The NS entropy versus EEG PSD profiles are shown for the FzP0, CzP0, F3Cz, C3C4, and FzC3 sensor combinations for (c) MT and (d) SPAN teams. The raw EEG PSD spectra are shown for MT teams (e) and SPAN teams F where the values for each PSD bin were averaged across the members of each team before generating the plots.

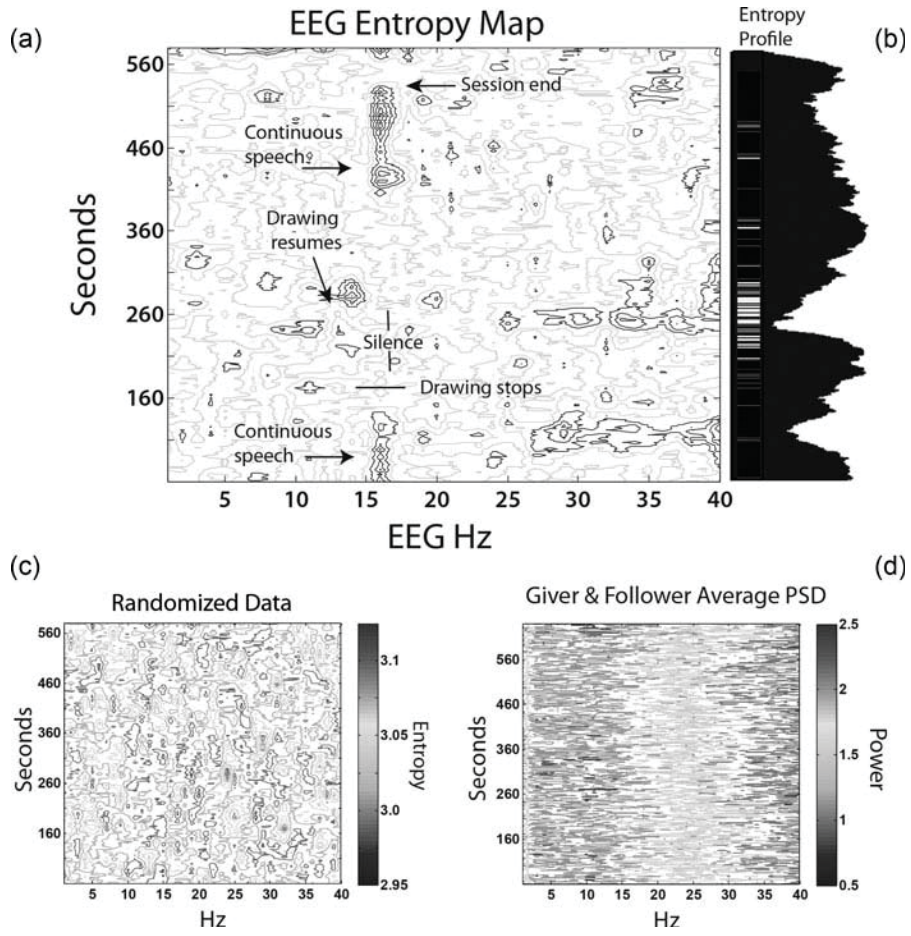

Figure 5. (a) Neurodynamic organizational models for the 1–40 Hz frequency channels were assembled into a three-dimensional temporal/frequency map. (b) An NS entropy profile was created of the performance by row-wise summation of the entropy values; the white bars indicate drawing mouse clicks. (c) The NS for each EEG PSD bin were randomized before calculating entropy levels and creating the neurodynamic organizational models. (d) The combined G and F EEG power values at each of the forty PSD frequency bins were averaged and plotted versus performance time.

and events as shown in Figure 5 for one MT team. The decreased 16 Hz NS entropy in this figure was seen during the first 2.5 min and in the last three minutes of the performance. The lowest overall NS entropy occurred during the 120 s interval when F had problems drawing (~160–280 s) (Figure 5b), which is shown by the concentrated mouse clicks around 260 s. This decrease in NS entropy was distributed across the ~25–40 Hz region, indicating that the task perturbation shifted the EEG frequencies where the team neurodynamic organizations occurred as well as increased the level of organization. As a control, the NS entropy calculations and three-dimensional mappings were created from the randomized 1–40 Hz NS symbol streams; this removed the NS entropy contours (Figure 5c). The team-combined and -averaged raw EEG PSD values for G and F also had little evidence of organizational structures (Figure 5d).

The MT is speech intensive that could produce artifacts in EEG alpha and beta frequencies (Friedman & Thayer, 1991). To determine whether speech induced periods of team neurodynamic organization in our tasks, an analysis of variance was conducted for three MT teams comparing NS entropy when G, F, or nobody was speaking. Between-group comparisons showed the lowest NS entropy when no one was speaking (no speech = 2.86 ± .37, (F speaking) = 2.92 ± .24, (G speaking) = 2.96 ± .23, $F = 16.5$, $df = 2$, $p < .001$). There were also multiple performances when there was low NS entropy while there was no speech (e.g., Figures 2 and 5), particularly when F had drawing problems. If speech effects

were present, they did not contribute to the increased neurodynamic organizations observed at the sampling rate of 1 Hz.

Mutual information: MT

NS entropy fluctuations identify periods of changing team neurodynamic organization but they provide little information about the possible roles that synergistic interactions among the team members play in these organizations. In the next studies, we compared the dynamics of MI expression with the dynamics of the NS entropy data streams and situated them within the changing events and activities of a MT performance (Figure 6). The MI values at 10, 16, and 38 Hz EEG bins are highlighted, as from Figure 4 the entropy-based neurodynamic organizations were the greatest around these frequency bins. The MI moving averages for one MT performance (Figure 6d and e) are displayed in the context of the F's drawing mouse clicks (Figure 6a), the speech periods of G and F (Figure 6b), the drawing transactions (Figure 6c), and the NS entropy profiles (Figure 6f). This was one of the lower performances (the map tracing is shown in Figure 1) where there were two major path deviations, one around 210–250 s, and one between 600 and 740 s. There was also a period between 400 and 500 s when F experienced problems navigating the mouse and was unable to draw lines; during this time there were repeated mouse clicks (Figure 6a) and little speech (Figure 6b). There were isolated periods of increased MI in each of the three EEG frequency bands; ~200–300 s and 500–600 s for 10 Hz MI, and ~425 s for 16 Hz MI. The 10 Hz MI was absent during the time of drawing difficulties, while most of the 16 Hz MI increase was during this time. There was one period of increased 38 Hz MI that occurred shortly after the period of drawing difficulties (~450 s).

A second comparison of the 10, 16, and 38 Hz MI and the average NS entropy dynamics is shown for the MT performance of a different team where F also had mouse-drawing difficulties at ~580–650 s (Figure 7).

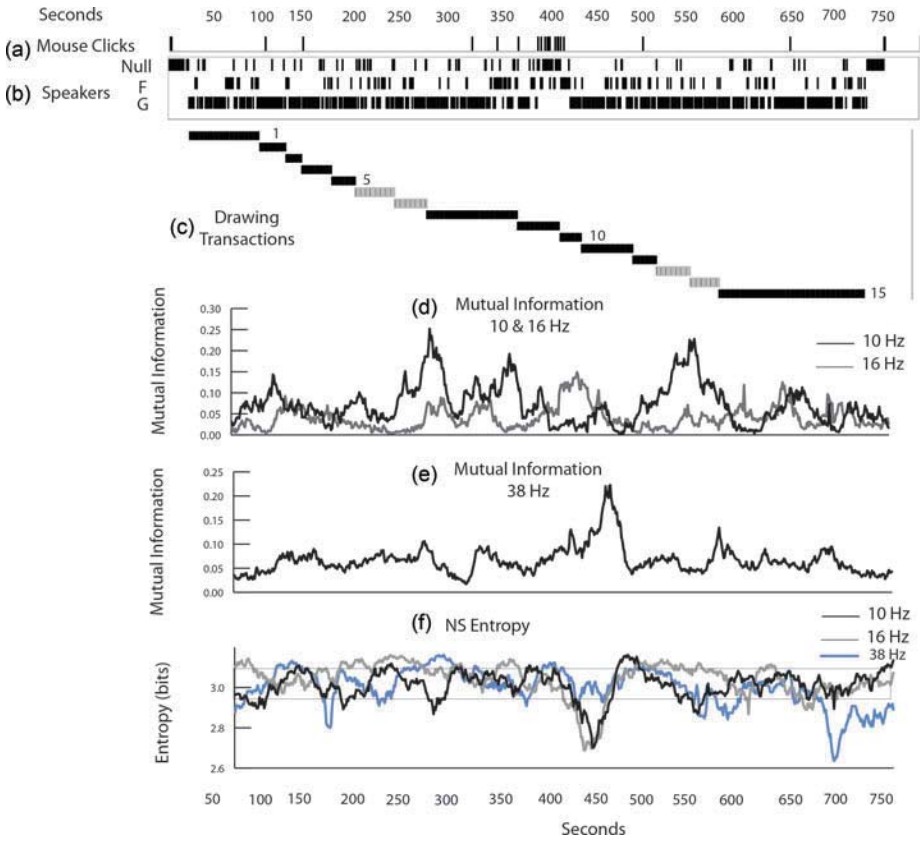

Figure 6. Linking NS entropy and mutual information with MT events and activities. The levels of the CzP0 10 Hz and 16 Hz NS entropy (f) and MI (d, e) are temporally aligned with the mouse clicks of the F (a), the speech periods of G and F (b), the transaction times for drawing segments (c).

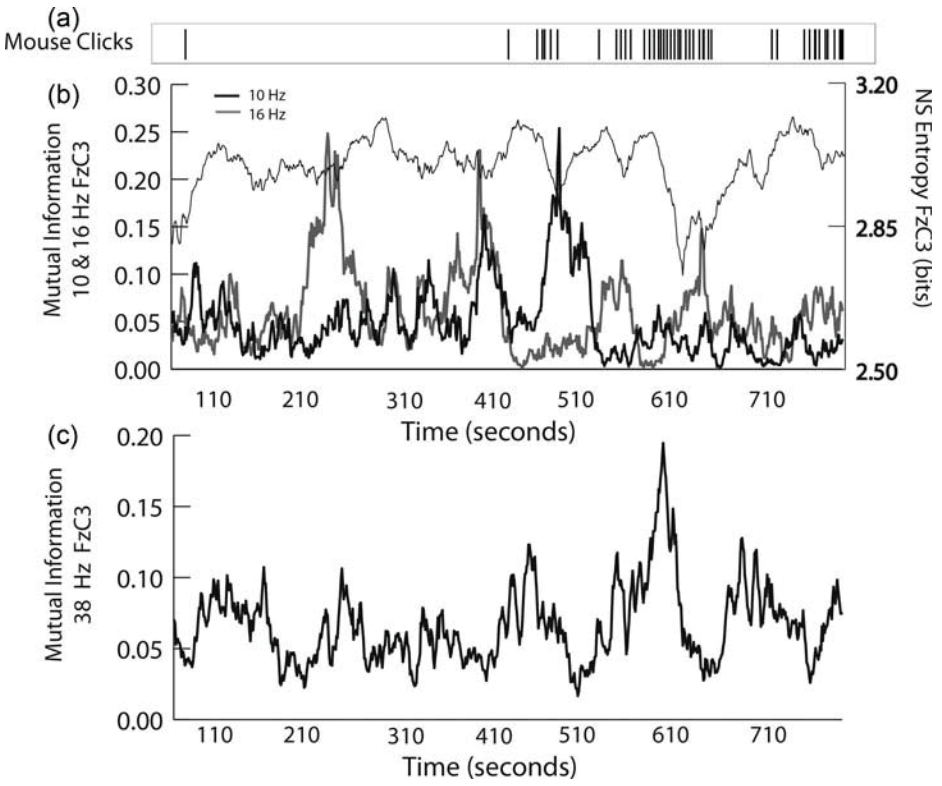

Figure 7. Linking mouse clicks with the 10, 16, and 38 Hz NS entropy and mutual information for a second MT performance.

There were two periods of increased 10 Hz MI between ~375 s and 525 s and two periods of 16 Hz MI, one of which coincided with the first period of increased 10 Hz MI. Similar to the performance in Figure 6, the NS entropy drop associated with the mouse-drawing problems showed low MI at the 10 Hz PSD band and a small increase in 16 Hz MI. There was a single 38 Hz MI peak, and this was present just before the period of F's drawing difficulties.

These results indicated that for the MT the periods of elevated MI did not occur continuously across all EEG frequencies but appeared intermittently and lasted ~45–60 s. For the most part, there was little overlap in the 10, 16, and 38 Hz MI peaks.

Neurodynamic entropy fluctuations during SPAN

The MT results showed (1) that most team neurodynamic organizations occurred around ~16–17 Hz and did not appear random; (2) the organizations were prolonged (2–4 min) and could be triggered by perturbations; and (3) similar plots of team-averaged raw EEG PSD frequency bin levels did not reveal these organizations. To expand the scope of this analytic approach, additional studies were conducted with five-person SPAN teams. In comparison with the ~16 Hz organizations observed during the MT, SPAN performances showed the greatest neurodynamic organizations at ~10 Hz (Figure 4b).

The briefing, scenario, and debriefing segments of SPAN constitute the top-level task structures. Each of these segments are lengthy (20–50+ min), and task effects on team organization should be most apparent across these segments. The levels of NS entropy were calculated across the 1–40 Hz EEG frequency bins and were significantly higher for the scenario than either the briefing or debriefing (F = 3.52, df = 2, p = .04) (Figure 8).

The neurodynamic entropy profiles across frequencies indicated the least neurodynamic organization (i.e., higher NS entropy) at the lower frequencies and progressively more organization (i.e., decreased NS entropy) toward the 40 Hz EEG band. In the three profiles, there was also a major region of team organization in the 8–13 Hz frequencies (i.e., the alpha region), which was greater in the debriefing segment when compared with the briefing or scenario (F = 7.88, df = 2, p = .002).

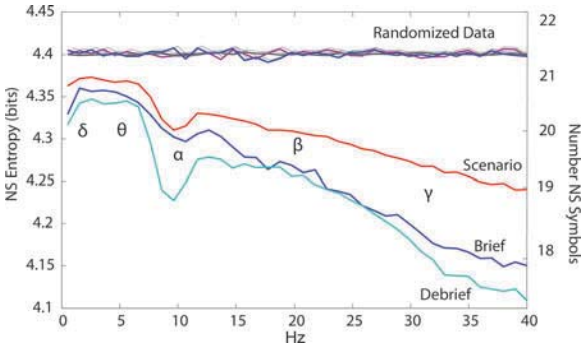

Figure 8. Frequency–entropy submarine piloting and navigation team profiles. The NS entropy streams from 10 submarine navigation performances were separated into the briefing, scenario, and debriefing segments and the frequency–entropy profiles were calculated. The EEG frequencies corresponding to the delta, theta, alpha, beta, and gamma ranges are indicated by Greek characters. Randomizing the data streams resulted in the NS entropy profiles at the top of the screen. The scale to the right translates the NS entropy levels into the number of symbols represented.

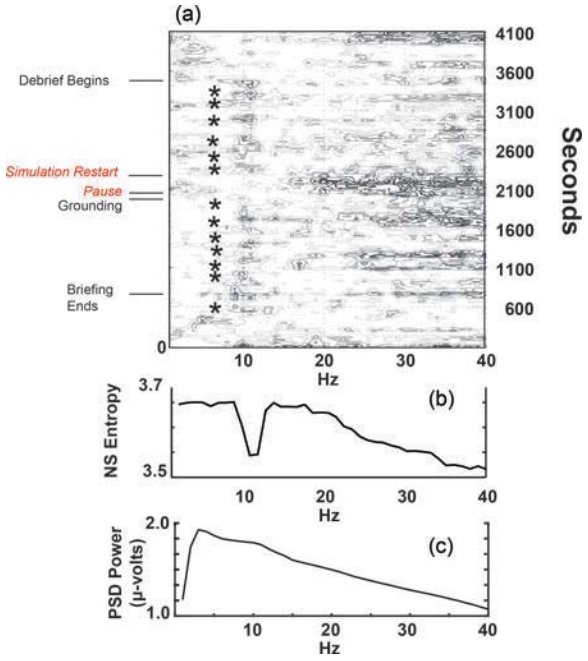

Figure 9. (a) NS entropy models were created for each of the 1–40 Hz frequencies of a SPAN team performance and assembled into a three-dimensional temporal/frequency entropy map. Significant events are labeled to the left, and the asterisks indicate the "mark rounds" calls. (b) The entropy values were summed column-wise creating a frequency–entropy histogram. (c) The raw EEG PSD spectrum was generated from the averaged values of each of the crew members.

Surrogate data testing was used in all experiments to determine whether the neurodynamic organizations were due to the sequential ordering of the symbols in the data streams. In this process, the NS symbol streams are randomly shuffled before performing the entropy calculations; this process resulted in a uniform higher level of entropy for the three training segments. The entropy values are based on the distribution of the 25 NS in the data streams, and the maximum entropy expected would be 4.64. The scale to the right of Figure 8 shows that following randomization the NS entropy level was 4.4 or ~22 symbols. The period of maximum organization in the debriefing was 4.1 or ~17 symbols, about a 25% change in team organization.

A temporal/frequency neurodynamic entropy map was created for one SPAN performance where there was an external perturbation when the instructor paused the simulation. The temporal/frequency map in Figure 9 showed that the 10 Hz fluctuations were absent during the debriefing and present in the scenario except for a period between 1800 and 2300 s. In the scenario, they appeared periodic and temporally aligned with the "rounds" cycles, which are marked in Figure 9a by the asterisks.

Between 1600 and 2000 s, the team had problems establishing the submarine's position due to instrument failures inserted by the instructor. These difficulties resulted in the instructor pausing the simulation to review the challenges (~2050 s). The 10 Hz neurodynamic organizations were absent until the simulation restarted (~2300 s). While the level of team organization in the 10 Hz PSD band declined during the break, there was increased organization in the ~15–40 Hz EEG PSD bins. This organization was most pronounced during the period leading to the simulation pause. This quantitative change in the NS entropy profile at 10 Hz was not reflected in the raw EEG PSD profile created by averaging the power values across the crew (Figure 9c).

The dynamical associations between the "rounds" cycles and the 10 Hz PSD team neurodynamic organizations were further explored in the 60 s interval between the "1 min to next round" and the "mark round" calls (Figure 10a). Across 10 "rounds" cycles selected before and after the instructor's pause, the NS entropy in the 10 s before the "mark rounds" call was significantly lower than that in the 10 s before the "1 min to next round" or the remaining seconds during the scenario ("mark rounds" = 3.45 ± 0.1 bits; "1 min to next round" = 3.59 ± 0.1 bits; remaining seconds = 3.50 ± 0.1 bits; $H = 56.1$, $df = 2$, $p < .001$; Kruskal–Wallis H test). As a control, when similar

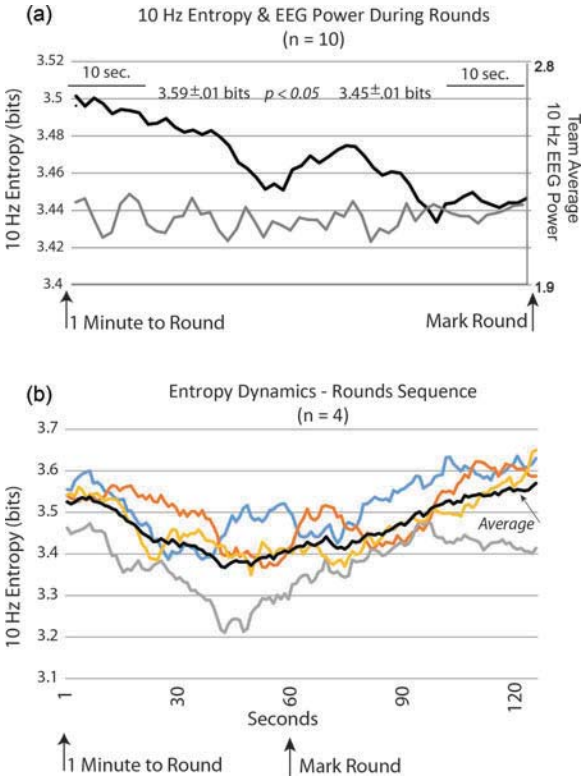

Figure 10. Dynamics of 10 Hz neurodynamic organizations during "rounds." (a) Ten "rounds" cycles were aligned with the "1 min to mark round" call and the mean 10 Hz NS entropy values were plotted each second until the "mark round" call. The gray line shows the average of the raw 10 Hz PSD power levels of the crew members. (b) The NS entropy was plotted for four "rounds" cycles with similar durations from the "mark round" to the "end round" calls.

comparisons were made using the NS entropy at the 20 Hz bin, they were not significantly different ($H = 2.8$, $df = 2$, $p = .24$).

We also compared the raw EEG 10 Hz PSD levels at 10 s before the "1 min to next rounds" call with those 10 s before the "mark rounds" call; the results were not significantly different ("1 min to next round" = 2.18 ± 0.07; "mark round" = 2.19 ± 0.02; $t = -0.35$, $df = 9$, $p = .73$). As expected from these results, the second-by-second profile of the team-averaged raw 10 Hz PSD showed no trends during the 60 s interval between the "1 min to next round" and "mark rounds" calls (Figure 10a).

The interval between "1 min to the mark round" and "mark round" calls was generally 60 s, while those from the "mark round" to "end round" calls varied from seconds to minutes depending on the accuracy of the fix. This variability complicated studying the postfix NS entropy dynamics with all "rounds" cycles. There were four "rounds" cycles where that interval approximated 60 s and these were used for the post "mark the round" modeling. In these intervals, the 10 Hz NS entropy values generally began rising 10–15 s before the "mark round" call and continued an upward trend for the next 60 s (Figure 10b).

Mutual information: SPAN

The NS entropy and MI comparisons for the MT G and F dyads indicated that temporal increases in MI occurred intermittently during a performance and were often aligned near periods of decreased NS entropy. The MT results in Figures 6 and 7 emphasized differences across EEG frequency bins at a single EEG sensor channel (either CzP0 or FzC3), and showed that MI increases could be found in the 10, 16, and 38 Hz EEG frequency bins.

We next extended the comparisons between NS entropy fluctuations and team MI levels to the SPAN performance that was highlighted in Figure 9. Rather than emphasize across EEG frequency differences, the studies in Figure 11 compared the averaged MI levels for all EEG frequencies for the different EEG sensor channels, i.e., FzP0, CzP0, FzC3, and C3C4. The across-sensor, across-frequency mean NS entropy for this performance is shown in Figure 11a with the periods of decreased NS entropy at ~1150, 1650, and 2100 s corresponding to the darkened contours in Figure 9.

Based on the NS entropy × EEG PSD frequency profiles shown in Figure 8, the different dyad MI calculations were performed using data combined from either the FzP0 and CzP0 sensors or the FzC3 and C3C4 sensor channels; also shown in Figure 11b is the NS entropy levels for these sensor channels.

Each of the six dyad combinations showed one or more periods of increased MI that generally lasted 45–90 s (Figure 11c–h). Across the different dyad combinations, there were MI spikes that closely aligned with one of the major drops in NS entropy.

DISCUSSION

Team rhythms can be thought of as emergent properties arising from team members performing individual tasks and sharing information with other team members. In this context, it is likely that team rhythms across scales from seconds to minutes contribute to what is behaviorally seen as the rhythm of a team. In line with Ashby's (1956) law of requisite variety, the rhythm of a team is always changing in response to

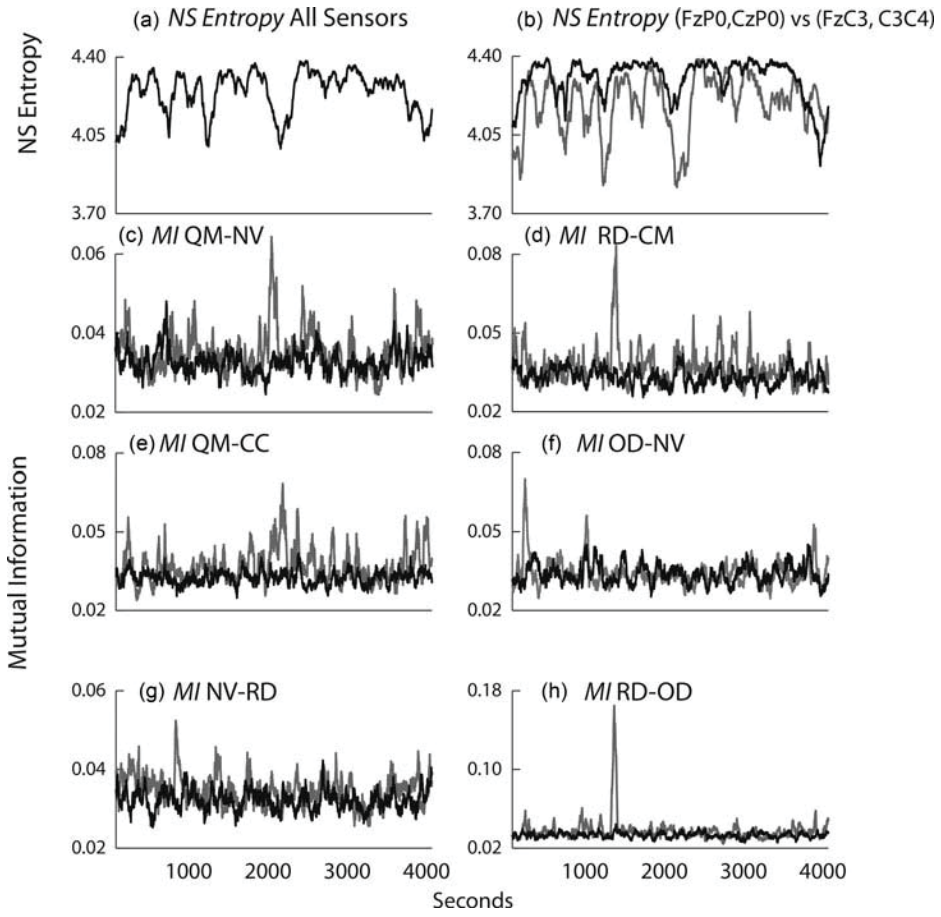

Figure 11. NS entropy and mutual information dynamics during submarine piloting and navigation. (a) The NS entropy levels were averaged for the 1–40 Hz frequency channels across the FzP0, CZP0, FzC3, and C3C4 EEG sensor channels. (b) The across-frequency NS entropy levels were averaged for the (FzP0 and CzP0) and (FzC3 and C3C4) channels and plotted versus time. (c–h) The mutual information was calculated for the (c) QM-NV, (d) RD-CM, (e) QM-CM, (d) OD-NV, (e) NV-RD, and the (h) RD-OD dyads; profiles are shown in each display for the averages at the FzP0 + CzP0 (black) or FzC3 + C3C4 (gray) channels.

the varying constraints imposed by the environment. When the challenges in the environmental landscape exceed the base level of complexity for the team's experience, then the overall team rhythm can be lost and the crew must work dynamically to reconfigure their interactions to establish new rhythms matched to the new constraints of the task. Identifying these periods of adaptive change could give a clearer picture of the antecedent events as well as the dynamical processes by which teams regain an operational rhythm.

This study describes an EEG-based hyperscanning approach for modeling these neurodynamic reorganizations in response to shifting task demands. Our operational definition of neurodynamic organization was when there were persistent (seconds to minutes) EEG PSD relationship(s) among some or all crew members. To detect these organizations, we developed a symbolic modeling system that scales across both team size and task complexity. For these studies, we chose to limit our modeling to simultaneous measurements across team members although there are well-known lead-lag relationships that occur during conversation and nonverbal mirroring (Ashenfelter, 2007). There is nothing to preclude such lagged modeling in the future, however.

During these neurodynamic organizations, the Shannon entropy of the NS symbol streams dropped as fewer of the potential neurodynamic symbol states were being expressed over a window of time. The simultaneous modeling of the 1–40 Hz EEG frequency bins across multiple sensor locations provided a coarse-grained analysis of the temporal changes in the neurodynamic organization of the teams that could be related to task events. The analysis also provided a

rapid way to relate these dynamics to previously described social coordination measures in the alpha and beta EEG regions (Tognoli & Kelso, 2013).

During both tasks, there was decreased NS entropy in most EEG frequency bins, although the decreases in the delta (0.5–3.5 Hz) and theta bands were small. This may be due in part to delta and theta rhythms being more associated with individual rather than team actions/activities. Delta oscillations are often associated with deep sleep, although more recent studies suggest a role in the inhibition of sensory stimuli that interfere with internal concentration (Harmony, 2013). Theta oscillations (~7 Hz) play important roles in what appear to be properties of individuals rather than teams, such as representing spatial information, predictive navigation, and memory encoding and retrieval (Battaglia, Sutherland, & McNaughton, 2004; O'Keefe & Dostrovsky, 1971).

The primary neurodynamic organizations of the MT teams were in the 15–17 Hz EEG frequency bins while the largest organizations occurred in SPAN teams in the 9–12 Hz bins. As both frequency ranges contain previously described social coordination markers, this was not surprising (Pineda, 2008; Tognoli & Kelso, 2013). More surprising was the apparent differential expressions of these synchronizations across the two tasks. The ~16 Hz organizational activity in MT teams was suggestive of mu rhythms, an index of pre-motor activity (Oberman et al., 2008; Pineda, 2008). Mu rhythms are characterized by an alpha component of ~8–13 Hz attributed to sensorimotor areas (S1 M1) and a beta component of ~15–20 Hz, which may link to anticipatory motor activities that are modulated by the direct observation and imagination of movement. Planning as well as the execution of hand movements desynchronize (i.e., suppress) these rhythms, while inhibition of motor behavior enhances their activity (Caetano, Jousmaki, & Hari, 2007; Menoret et al., 2014). Mu rhythms may be present and modulated during the MT as a result of the hand gestures that were often exchanged when the face-to-face dyads communicated the relationships of the path/landmarks to one another.

The dynamics of the ~10 Hz expression in SPAN teams presented a different coordination picture. The ~10 Hz NS entropy decreases were greatest in the debriefing segment of SPAN, where the crew takes turns reviewing the session from their perspective and responding to the instructor's comments; there was seldom more than one person speaking at a time. The decreases in 10 Hz NS entropy were less in the briefing when the team members calibrated their instruments and conducted an initial "round" to establish the ship's starting position. The 10 Hz NS entropy was highest in the scenario with at least a portion of the neurodynamic organization resulting from the coordinated activity of periodically establishing the ship's position. Although alpha rhythms have multiple topological origins in the brain, the limited number of EEG sensors used for data collection precluded a more detailed differential description of alpha band dynamics.

We were surprised to find that the largest neurodynamic organizations occurred in the 35–40 Hz EEG bins as we are not aware of other descriptions of gamma band synchronizations during social coordination. As gamma oscillations are often short-lived, the neurodynamic organizations observed may be examples of coincidental synchrony or perhaps cross-frequency coupling with other EEG frequencies. Such couplings between alpha and gamma have been implicated in the maintenance of information in working memory (Palva & Palva, 2007; Roux & Uhlhaas, 2014). In this regard, the gamma band neurodynamic organizations often occurred around unexpected task disturbances (i.e., drawing difficulties in MT and the pause of the simulation for SPAN).

Describing the role of these neurodynamic organizations with regard to team function, performance, and synchrony depends in part on relating the neurodynamic organizations identified by changes in NS entropy with ideas on the form(s) of synchrony being observed. Burgess (2013) recently distinguished four different forms of across-system synchronizations that have relevance for hyperscanning studies. These include coincidental synchrony when noncoupled events occur simultaneously, an example being checkout lines in a store; external entrainment, an example being musicians playing in time to a metronome; driven synchrony where the behavior of one individual drives the behavior of others, i.e., an audience listening to a lecture; and reciprocal synchronization as seen in the repetitive speaker–listener couplings described by Baess et al. (2012) and Dumas, Nadel, Soussignan, Martinerie, and Garnero (2010).

The fluctuations in the NS entropy identify periods of changing team neurodynamic organization, but they provide little information about the possible roles that synchronous interactions among the team members played in these organizations. To better situate NS entropy changes into a model of team information flows, we determined the mutual dependence of the EEG PSD levels (i.e., MI) for dyads within the experimental teams.

The MT studies in Figures 6 and 7 examined MI expression at different EEG frequency bins for a single EEG sensor channel, and periods of elevated MI were seen within the 10, 16, and 38 Hz PSD bins.

Unlike the more continuous fluctuations seen in NS entropy that evolved over several minutes, the elevated MI levels were shorter (~45–60 s) and more isolated.

The five-person submarine navigation teams are more complex due to the number of possible dyad combinations. To simplify the exploration of the MI dynamics across these dyads, we averaged the MI across the 1–40 Hz frequency spectrum and displayed the NS entropy profiles for the combined values of the FzP0 + CzP0 channels and the FzC3 + C3C4 channels. Aggregating the data in this way seemed a reasonable first approximation from the differential NS entropy levels seen across the different EED channels shown in Figure 4. While there were a limited number of MI peaks for each dyad, these were often aligned with periods of decreased NS entropy.

The differential dynamics of MI and NS entropy may provide different avenues for training and future research. NS entropy fluctuations can provide a rapid overview of team dynamics that could be a useful adjunct for team training. Capturing the frequency, magnitude, and duration of the times when teams neurodynamically reorganize could help instructors not only quantitatively infer the skill level of a team but also identify situations when the team was challenged, providing targets for future training activities. While NS entropy does not provide immediate details as to the nature of the reorganizations, this information can be derived by inspection of the NS symbol expressions and state diagrams.

The finer granularity of MI, on the other hand, would enable more precise temporal comparisons with other measures of teamwork like speech (Gorman, Martin, Dunbar, Stevens, & Galloway, 2013). The MI expressions in larger teams with multiple dyad combinations may provide ways for tracking interaction flows throughout teams. This is illustrated in Figure 12 where the maximum MI for the QM-NV and QM-CC dyads appear temporally embedded within a larger NS entropy fluctuation.

In this regard, NS entropy may be a "slow" variable in the sense that it integrates multiple more microscopic processes, here illustrated for MI. In other social systems, slow variables serve as better predictors of the local future configuration of a system than the states of the fluctuating more microscopic components (Flack, 2012). In this way, we can begin to think about modeling networks of information flows that span different scales of teamwork (Villaverde et al., 2014).

One approach toward building these models would draw from the work on neuronal population codes that have been used to study how spike trains encode

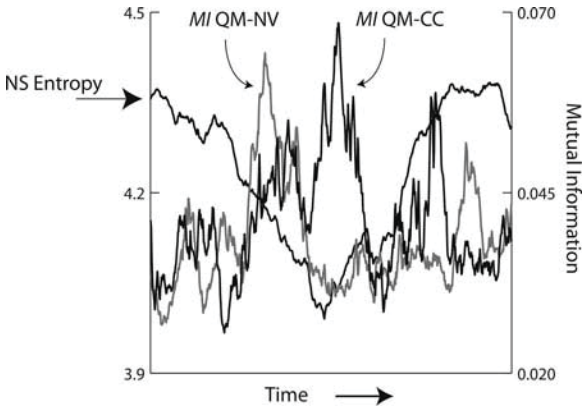

Figure 12. Dynamics of NS entropy and mutual information. This figure expands the NS entropy drop between 1850 and 2350 s shown in Figure 11, with overlays of the MI values for the QM-NV and QM-CC dyads. The increased MI calculated from the QM-NV dyad was maximum at 2072 s while the MI calculated from the QM-CC dyad was maximum at 2217s.

sensory variables (Onken et al., 2014; Quiroga & Panzeri, 2009; Schneidman et al., 2003). These studies have used MI approaches to capture information flows from populations of neurons under stimulus-repeat and single-trial experimental paradigms. For teaming studies, the MI from different dyads, from different EEG channels and different frequency bins might be viewed as "spike trains" from which team information might be similarly extracted, analyzed, and quantified.

With defined symbol spaces, quantitative descriptions can be made about the neurodynamic organizations of teams in shifting environmental landscapes, whether these charges are abrupt like those associated with major shifts in the segments of the task like briefing, scenario, and debriefing for submarine teams or when teams become challenged by external perturbations. The NS entropy and MI measures also simplify quantitative comparisons across teams or over time across training sessions, expanding our understanding of team dynamics in natural settings by identifying the types of events that trigger team reorganizations.

Original manuscript received 19 December 2014
Revised manuscript accepted 27 May 2015
First published online 22 June 2015

REFERENCES

Adrian, D., & Matthews, B. H. C. (1934). The Berger rhythm: Potential changes from the occipital lobes in man. *Brain*, *57*, 355–385. doi:10.1093/brain/57.4.355

Ashby, R. W. (1956). *An introduction to cybernetics*. London: Methuen.

Ashenfelter, K. (2007) *Simultaneous analysis of verbal and nonverbal data during conversation: symmetry and turn-taking* (Unpublished thesis). South Bend, IN: University of Notre Dame.

Baess, P., Zhdanov, A., Mandel, A., Parkkonen, L., Hirvenkari, L., Mäkelä, J. P., … Hari, R. (2012). MEG dual scanning: A procedure to study real-time auditory interaction between two persons. *Frontiers in Human Neuroscience*, *6*. doi:10.3389/fnhum.2012.00083

Battaglia, F. P., Sutherland, G. R., & McNaughton, B. L. (2004). Local sensory cues and place cell directionality: Additional evidence of prospective coding in the hippocampus. *Journal of Neuroscience*, *24*, 4541–4550. doi:10.1523/JNEUROSCI.4896-03.2004

Berka, C., Levendowski, D. J., Cvetinovic, M. M., Petrovic, M. M., Davis, G., & Luminaco, M. (2004). Real- time analysis of EEG indexes of alertness, cognition, and memory acquired with a wireless EEG headset. *International Journal of Human-Computer Interaction*, *17*(2), 151–170. doi:10.1207/s15327590ijhc1702_3

Burgess, A. P. (2013). On the interpretation of synchronization in EEG hyperscanning studies: A cautionary note. *Frontiers in Human Neuroscience*, *7*(Article 881). doi:10.3389/fnhum.2013.00881

Caetano, G., Jousmaki, V., & Hari, R. (2007). Actor's and observers primary motor cortices stabilize similarly after seen or heard motor actions. *Proceedings of the National Academy of Sciences*, *104*, 9058–9062. doi:10.1073/pnas.0702453104

Canolty, R. T., Edwards, E., Dalal, S. S., Soltani, M., Nagarajan, S. S., Kirsch, H. E., … Knight, R. T. (2006). High gamma power is phase-locked to theta oscillations in human neocortex. *Science*, *313*, 1626–1628. doi:10.1126/science.1128115

Daw, C. S., Finney, C. E. A., & Tracy, E. R. (2003). A review of symbolic analysis of experimental data. *Review of Scientific Instruments*, *74*, 915.

Doherty-Sneddon, G., Anderson, A., O'Malley, C., Langton, S., Garrod, S., & Bruce, V. (1997). Face-to-face and video-mediated communication: A comparison of dialogue structure and task performance. *Journal of Experimental Psychology Applied*, *3*(2), 105–125.

Dumas, G., Nadel, J., Soussignan, R., Martinerie, J., & Garnero, L. (2010). Inter-brain synchronization during social interaction. *PLoS One*, *5*, 12116. doi:10.1371/journal.pone.0012166

Fishel, S. R., Muth, E. R., & Hoover, A. W. (2007). Establishing appropriate physiological baseline procedures for real-time physiological measurement. *Journal of Cognitive Engineering and Decision Making*, *1*, 286–308. doi:10.1518/155534307X255636

Flack, J. C. (2012). Multiple time-scales and the developmental dynamics of social systems. *Philosophical Transactions of the Royal Society B: Biological Sciences*, *367*, 1802–1810. doi:10.1098/rstb.2011.0214

Friedman, B. H., & Thayer, J. F. (1991). Facial muscle activity and EEG recordings: Redundancy analysis. *Electroencephalography and Clinical Neurophysiology*, *79*, 358–360. doi:10.1016/0013-4694(91)90200-N

Fries, P. (2005). A mechanism for cognitive dynamics: Neuronal communication through neuronal coherence. *Trends in Cognitive Sciences*, *9*, 474–480. doi:10.1016/j.tics.2005.08.011

Galambos, R., Makeig, S., & Talmachoff, P. (1981). A 40 Hz auditory potential recorded from the human scalp. *Proceedings of the National Academy of Sciences*, USA. *78*(4), 2643–2647. doi:10.1073/pnas.78.4.2643

Gorman, J. C., Amazeen, P. G., & Cooke, N. J. (2010). Team coordination dynamics. *Nonlinear Dynamics, Psychology, & Life Sciences*, *14*, 265–289.

Gorman, J. C., Martin, M. J., Dunbar, T. A., Stevens, R. H., & Galloway, T. (2013). Analysis of semantic content and its relation to team neurophysiology during submarine crew training. *Foundations of Augmented Cognition, Lecture Notes in Computer Science*, *8027*, 143–152.

Harmony, T. (2013). The functional significance of delta oscillations in cognitive processing. *Frontiers in Integrative Neurosciences*, *7*(article 83). doi:10.3389/fnint.2013.00083

Hasson, U., Ghazanfar, A., Glantucci, B., Garrod, S., & Keysers, C. (2011). Brain-to-brain coupling: A mechanism for creating and sharing a social world. *Trends in Cognitive Sciences*, *17*, 413–425.

Hasson, U., Nir, Y., Levy, I., Fuhrmann, G., & Malach, R. (2004). Intersubject synchronization of cortical activity during natural vision. *Science*, *303*, 1634–1640. doi:10.1126/science.1089506

Hollnagel, E. (2009). The four cornerstones of resilience engineering. In E. Hollnagel & S. Dekker (Eds.), *Resilience engineering perspectives: Vol 2. Preparation and restoration* (pp. 117–133). Farnham: Ashgate.

Kolm, J., Stevens, R., & Galloway, T. (2013). How long is the coastline for teamwork? In *Presented at 15th international conference on human-computer interaction: Augmented cognition*, Las Vegas, NV. Heidelberg: Springer.

Lin, J., Keogh, E., Lonardi, S., & Chiu, B. (2003, June 13). A symbolic representation of time series with implications for streaming algorithms. In *Proceedings of the 8th Data Mining and Knowledge Discovery*, San Diego, CA. New York, NY: Association for Computing Machines.

Menoret, M., Varnet, L., Fargier, R., Cheylus, A., Curie, A., Des Portes, V., … Paulignan, U. (2014). Neural correlates of non-verbal social interactions: A dual-EEG study. *Neurophyschologia*, *55*, 85–91.

Moreno, I., De Vega, M., & León, I. (2013). Understanding action language modulates oscillatory mu and beta rhythms in the same way as observing actions. *Brain and Cognition*, *82*(3), 236–242. doi:10.1016/j.bandc.2013.04.010

Oberman, L. M., Pineda, J. A., & Ramachandran, V. S. (2008). The human mirror neuron system: A link between action observation and social skills. *Social Cognitive and Affective Neuroscience*, *2*, 62–66. doi:10.1093/scan/nsl022

O'Keefe, J., & Dostrovsky, J. (1971). The hippocampus as a spatial map. Preliminary evidence from unit activity in the freely-moving rat. *Brain Research*, *34*, 171–175. doi:10.1016/0006-8993(71)90358-1

Onken, A., Chamanthi, P. P., Karunasekara, R., Kayser, C., & Panzeri, S. (2014). Understanding neural population coding: Information theoretic insights from the auditory

system. *Advances in Neuroscience*, *2014*(Article 907851). doi:10.1155/2014/907851

Palva, S., & Palva, J. M. (2007). New vistas for α-frequency band oscillations. *Trends in Neurosciences*, *30* (4), 150–158. doi:10.1016/j.tins.2007.02.001

Pineda, J. A. (2008). Sensorimotor cortex as a critical component of an 'extended' mirror neuron system: Does it solve the development, correspondence, and control problems in mirroring? *Behavioral and Brain Functions*, *4*, 47–63.

Quiroga, R. Q., & Panzeri, S. (2009). Extracting information from neuronal populations: Information theory and decoding approaches. *Nature Reviews Neuroscience*, *10*, 173–185. doi:10.1038/nrn2578

Roux, F., & Uhlhaas, P. (2014). Working memory and neural oscillations: Alpha-gamma versus theta-gamma codes for distinct WM information? *Trends in Cognitive Sciences*, *18*, 16–25. doi:10.1016/j.tics.2013.10.010

Salas, E., Stagl, K. C., & Burke, C. S. (2004). 25 Years of team effectiveness in organizations: Research themes and emerging needs. In C. L. Cooper & I. T. Robertson (Eds.), *International Review of Industrial and Organizational Psychology* (pp. 56–101). Hoboken, NJ: John Wiley & Sons.

Schneidman, E., Bialek, W., & Berry II, M. J. (2003). Synergy, redundancy, and independence in population codes. *Journal of Neuroscience*, *23*, 11539–11533.

Shannon, C., & Weaver, W. (1949). *The mathematical theory of communication*. Urbana: University of Illinois Press.

Stevens, R., Galloway, T., Wang, P., Berka, C., & Behneman, A. (2011). *Developing systems for the rapid modeling of team neurodynamics*. Interservice/Industry Training Simulation and Education Conference (I/ITSEC) 2011. Paper No. 11097.

Stevens, R. H., & Galloway, T. (2014). Toward a quantitative description of the neurodynamic organizations of teams. *Social Neuroscience*, *9*(2), 160–173. doi:10.1080/17470919.2014.883324

Stevens, R. H., Galloway, T., Wang, P., & Berka, C. (2012). Cognitive Neurophysiologic Synchronies: What Can They Contribute to the Study of Teamwork? *Human Factors: The Journal of the Human Factors and Ergonomics Society*, *54*, 489–502. doi:10.1177/0018720811427296

Stevens, R. H., Galloway, T., Wang, P., Berka, C., Tan, V., Wohlgemuth, T., … Buckles, R. (2012). Modeling the neurodynamic complexity of submarine navigation teams. *The Journal of Computational and Mathematical Organization Theory*, *9*, 346–369.

Stevens, R. H., Gorman, J. C., Amazeen, P., Likens, A., & Galloway, T. (2013). The organizational neurodynamics of teams. *Nonlinear Dynamics, Psychology and Life Sciences*, *17*(1), 67–86.

Tognoli, E., & Kelso, J. A. (2013). The coordination dynamics of social neuromarkers. Bibliographic Code: 2013arXiv1310.7275T.

Tognoli, E., Lagarde, J., De Guzman, G. C., & Kelso, J. A. S. (2007). The phi-complex as a neuromarker of human social coordination. *Proceedings of the National Academy of Sciences*, *104*, 8190–8195. doi:10.1073/pnas.0611453104

Van Noorden, L., & Moelants, D. (1999). Resonance in the perception of musical pulse. *Journal of New Music Research*, *28*(1), 43–66. doi:10.1076/jnmr.28.1.43.3122

Villaverde, A. F., Ross, J., Moran, F., & Banga, J. (2014). MIDER: Network inference with mutual information distance and entropy reduction. *Plos One*, *9*(5), e96732.

Wang, Y., Hong, B., Gao, X., & Gao, S. (2007). Design of electrode layout for motor imagery based brain-computer interface. *Electronics Letters*, *43*(10), 557–558.

Wildman, J., Salas, E., & Scott, C. (2014). Measuring cognition in teams: A cross-domain review. *Human Factors: The Journal of the Human Factors and Ergonomics Society*, *56*(5), 911–941. doi:10.1177/0018720813515907

Will, U., & Berg, E. (2007). Brain wave synchronization and entrainment to periodic acoustic stimuli. *Neuroscience Letters*, *424*, 55–60. doi:10.1016/j.neulet.2007.07.036